# Reversible acetylation regulates acetate and propionate metabolism in *Mycobacterium smegmatis*

Jennifer D. Hayden,[1] Lanisha R. Brown,[1] Harsha P. Gunawardena,[2] Ellen F. Perkowski,[1] Xian Chen[2] and Miriam Braunstein[1]

[1]Department of Microbiology and Immunology, School of Medicine, University of North Carolina, Chapel Hill, NC 27599, USA

[2]Department of Biochemistry and Biophysics, School of Medicine, University of North Carolina, Chapel Hill, NC 27599, USA

Correspondence
Miriam Braunstein
braunste@med.unc.edu

Received 12 April 2013
Accepted 25 June 2013

Carbon metabolic pathways are important to the pathogenesis of *Mycobacterium tuberculosis*, the causative agent of tuberculosis. However, extremely little is known about metabolic regulation in mycobacteria. There is growing evidence for lysine acetylation being a mechanism of regulating bacterial metabolism. Lysine acetylation is a post-translational modification in which an acetyl group is covalently attached to the side chain of a lysine residue. This modification is mediated by acetyltransferases, which add acetyl groups, and deacetylases, which remove the acetyl groups. Here we set out to test whether lysine acetylation and deacetylation impact acetate metabolism in the model mycobacteria *Mycobacterium smegmatis*, which possesses 25 candidate acetyltransferases and 3 putative lysine deacetylases. Using mutants lacking predicted acetyltransferases and deacetylases we showed that acetate metabolism in *M. smegmatis* is regulated by reversible acetylation of acetyl-CoA synthetase (Ms-Acs) through the action of a single pair of enzymes: the acetyltransferase Ms-PatA and the sirtuin deacetylase Ms-SrtN. We also confirmed that the role of Ms-PatA in regulating Ms-Acs regulation depends on cAMP binding. We additionally demonstrated a role for Ms-Acs, Ms-PatA and Ms-SrtN in regulating the metabolism of propionate in *M. smegmatis*. Finally, along with Ms-Acs, we identified a candidate propionyl-CoA synthetase, Ms5404, as acetylated in whole-cell lysates. This work lays the foundation for studying the regulatory circuit of acetylation and deacetylation in the cellular context of mycobacteria.

## INTRODUCTION

Lysine acetylation is a reversible post-translational modification (PTM) where an acetyl group is added to the side chain of a lysine residue. Much like phosphorylation, acetylation is an efficient and dynamic way to both positively and negatively regulate protein function. This modification is extensively studied in eukaryotes, especially with regard to its role in histone modifications. So far in prokaryotes, there are only a few examples of proteins regulated by lysine acetylation (Barak *et al.*, 1992; Lima *et al.*, 2011, 2012; Ramakrishnan *et al.*, 1998; Thao *et al.*, 2010; Yan *et al.*, 2008), with the best-characterized acetylated protein being acetyl-CoA synthetase (Acs) (Barak *et al.*, 2004; Starai *et al.*, 2002). However, it is likely that many more bacterial proteins are regulated by lysine acetylation. Proteomic studies identified between 100 and 200 proteins with acetylated lysine residues in *Escherichia coli*, *Salmonella enterica*, *Erwinia amylovora* and *Bacillus subtilis* (Kim *et al.*, 2013; Wang *et al.*, 2010; Wu *et al.*, 2013; Yu *et al.*, 2008; Zhang *et al.*, 2009). These proteins have functions in various processes; however, metabolic enzymes are the largest class of acetylated proteins identified in these studies.

*Mycobacterium tuberculosis* is the causative agent of tuberculosis disease, which is responsible for 1.4 million deaths per year (WHO, 2013). New drugs are needed to control drug-resistant *M. tuberculosis* infections, and a more complete understanding of *M. tuberculosis* biology will guide such efforts. It is clear that the carbon metabolic pathways of *M. tuberculosis* are critical to the growth and persistence of this pathogen in the host (Marrero *et al.*,

Abbreviations: AUC, area under the curve; FDR, false discovery rate; GNAT, Gcn5-related *N*-acetyltransferase; LC, liquid chromatography; PTM, post-translational modification; RFU, relative fluorescence units; XIC, extracted ion chromatogram.

Two supplementary figures and a supplementary table are available with the online version of this paper.

 

2010; McKinney *et al.*, 2000; Muñoz-Elías & McKinney, 2005; Rhee *et al.*, 2011). The ability of *M. tuberculosis* to adapt its metabolism throughout infection is also believed to be important (Eisenreich *et al.*, 2010; Muñoz-Elías & McKinney, 2006; Rhee *et al.*, 2011). However, extremely little is known about metabolic regulation in any mycobacteria.

In this study, we investigated the biological consequence of acetylation of Acs in the model mycobacterial species *Mycobacterium smegmatis*. Acs converts the short chain fatty acid acetate to acetyl-CoA, a central molecule in many metabolic processes including the tricarboxylic acid cycle. While there have been no prior studies of Δ*acs* mutants of mycobacteria, analysis of Δ*acs* mutants of other bacteria demonstrates a role for Acs in enabling growth when a low concentration of acetate is present as the sole carbon source (Castaño-Cerezo *et al.*, 2011; Gardner & Escalante-Semerena, 2009; Kumari *et al.*, 1995; Starai *et al.*, 2003). The biological impact of reversible Acs acetylation has been investigated in a small collection of bacteria, with the *S. enterica* enzyme being one of the best-studied examples (Barak *et al.*, 2004; Castaño-Cerezo *et al.*, 2011; Crosby *et al.*, 2010; Gardner *et al.*, 2006). In *S. enterica*, Acs is acetylated by protein acetyltransferase (Pat), a Gcn5-related *N*-acetyltransferase (GNAT) (Starai & Escalante-Semerena, 2004). This acetylation inhibits Acs function (Fig. 1a) (Starai & Escalante-Semerena, 2004). In *S. enterica*, the deacetylase CobB removes the acetyl group, allowing Acs to regain activity (Fig. 1a) (Starai *et al.*, 2002). CobB is a member of the $NAD^+$-dependent sirtuin, or class III, family of deacetylases. In *B. subtilis*, there are two deacetylases involved in Acs regulation: a sirtuin SrtN and a Zn-dependent class I deacetylase AcuC (Gardner & Escalante-Semerena, 2009).

Lysine acetylation has been detected in mycobacteria by anti-acetyl lysine Western blot (Nambi *et al.*, 2010). Furthermore, inspection of mycobacterial genomes reveals genes encoding Acs and candidate lysine acetyltransferases and deacetylases, including a large number of predicted GNATs: 25 in *M. smegmatis* and 20 in *M. tuberculosis* (UniProt Consortium, 2012). *In vitro* studies show that the *M. smegmatis* Pat protein (Ms5458, Ms-PatA) and the *M. tuberculosis* Pat (Rv0998, Mt-PatA), which share amino acid homology with the *S. enterica* Pat, can acetylate purified *M. tuberculosis* Acs (Rv3667, Mt-Acs) (Xu *et al.*, 2011). Mt-PatA has also been referred to as KATmt (Nambi *et al.*, 2013). *In vitro* studies further demonstrate that acetylated Mt-Acs can be deacetylated by the *M. tuberculosis* Rv1151c protein or by its *M. smegmatis* orthologue Ms5175 (Gu *et al.*, 2009; Li *et al.*, 2011a; Xu *et al.*, 2011). We refer to Rv1151c as Mt-SrtN because it is the only predicted sirtuin deacetylase of *M. tuberculosis*, and we call Ms5175 Ms-SrtN. There are, however, multiple predicted deacetylases in *M. smegmatis*: two predicted sirtuins, Ms5175 and Ms4620, and a putative Zn-dependent class I deacetylase, Ms0171 (Fig. 1b).

*In vitro* studies argue that lysine acetylation regulates mycobacterial Acs. However, in the context of the mycobacterial cell the importance of lysine acetylation and deacetylation to Acs and acetate metabolism has never been demonstrated. Here, we carried out a phenotypic analysis of *M. smegmatis* mutants lacking predicted acetyltransferases and deacetylases, and showed that a single pair of enzymes, Ms-PatA and Ms-SrtN, regulates acetate metabolism, as well as propionate metabolism. Mycobacterial Pat proteins are unusual in containing a cAMP-binding domain, which is required for their function *in vitro* (Lee *et al.*, 2012; Nambi *et al.*, 2010; Xu *et al.*, 2011). In our study, we confirmed that Ms-PatA requires cAMP binding in cells. Finally, along with Acs, we identified the predicted propionyl-CoA synthetase Ms5404 as being acetylated in *M. smegmatis*.

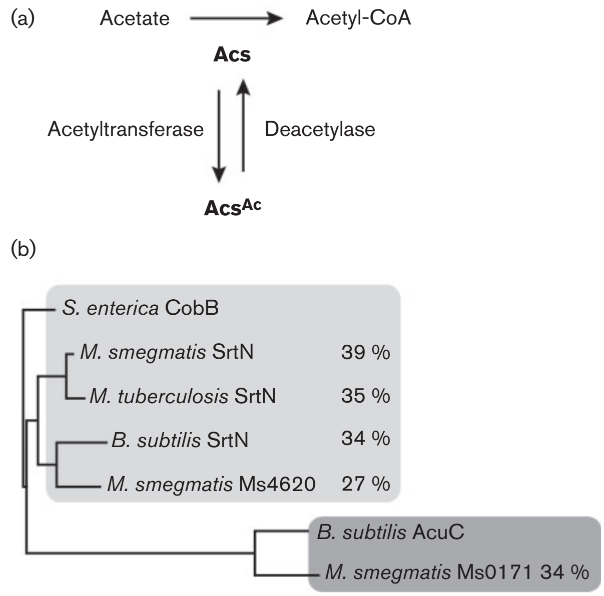


**Fig. 1.** Model of Acs function and regulation. (a) Acs performs the first step of acetate metabolism by converting acetate to acetyl-CoA. Acs can be lysine acetylated ($Acs^{Ac}$) by acetyltransferases, which causes Acs to become inactive. The acetyl group can be removed by deacetylases, allowing Acs to again convert acetate to acetyl-CoA. (b) Phylogenetic tree of selected bacterial deacetylases. An unrooted phylogenetic tree was created using PATRIC (Gillespie *et al.*, 2011). The light grey box indicates the sirtuin family of deacetylases, where numbers after each protein display percent sequence similarity to *S. enterica* CobB. The mycobacterial SrtN proteins group together and are the most closely related to *S. enterica* CobB. Selected class I deacetylases are shown in the dark grey box and the number after Ms0171 indicates percent sequence similarity to *B. subtilis* AcuC. As expected, the class I deacetylases form their own branch of the tree.

## METHODS

**Bacterial strains and growth conditions.** For genetic manipulations, *M. smegmatis* $mc^2155$ was grown in 7H9 (Difco) with 0.5 % glucose, 0.2 % glycerol and 0.1 % tyloxapol (Sigma), and grown at

37 °C. For growth curves, cultures were grown in M9 media (12.6 mM $Na_2HPO_4$, 22 mM $KH_2PO_4$, 8 mM NaCl, 19 mM $NH_4Cl$, 2 mM $MgSO_4$, 0.1 mM $CaCl_2$) with 0.1 % tyloxapol. Provided carbon sources included 0.5 % glucose and 0.2 % glycerol, 2.5 mM sodium acetate, or 2.5 mM sodium propionate. To enumerate c.f.u., cultures were diluted and plated on 7H10 (Difco) with 0.5 % glucose, 0.2 % glycerol and 0.1 % tyloxapol. When needed, antibiotics were used at the following concentrations: 20 μg $ml^{-1}$ kanamycin, 50 μg $ml^{-1}$ hygromycin. DH5α *E. coli* was grown in LB broth (Fisher Scientific) with the following antibiotics when necessary: 40 μg $ml^{-1}$ kanamycin, 150 μg $ml^{-1}$ hygromycin, 100 μg $ml^{-1}$ ampicillin.

**Mutant construction.** *M. smegmatis* mutants were constructed via recombineering (van Kessel & Hatfull, 2008; van Kessel *et al.*, 2008). Briefly, allelic exchange vectors were constructed by cloning 500–800 bp upstream and downstream flanks of the target gene (see Table S1, available in *Microbiology* Online, for primer information) on either side of a hygromycin-resistance cassette in pMP614 (a kind gift from Martin Pavelka, University of Rochester Medical Center, Rochester, NY, USA). The resulting vector was linearized by digesting with *Xba*I and *Kpn*I, and was used to transform *M. smegmatis* $mc^2155$ harbouring the multicopy Kan-marked plasmid pJV53, which encodes the phage-derived recombinase genes needed for recombination of linear DNA. Recombinase expression from pJV53 was induced by a 3 h incubation with 0.2 % acetamide. Following induction, electrocompetent cells were prepared and transformed with the linearized allelic exchange vectors (Snapper *et al.*, 1990). All mutants were confirmed by Southern blot analysis (data not shown). Confirmed mutant strains were cured of plasmid pJV53 by growing cultures to saturation without antibiotic and screening for kanamycin-sensitive colonies. To engineer multiple deletions in the same strain, the hygromycin-resistance gene was removed via resolvase recognition sites using pMP854, which expresses TnpR resolvase (a kind gift from Martin Pavelka). pMP854 was later cured from the deletion strains. A complete strain list is found in Table 1 and plasmids are listed in Table 2.

**Complementation vector construction.** To complement mutations, the gene of interest was amplified by PCR (see Table S1 for primer information) and cloned into pCR2.1 by TA cloning (Invitrogen). The resulting vectors were sequenced to verify the genes were error-free, and then digested with *Msc*I and *Hin*dIII (for pJH33 and pJH40) or *Sma*I and *Hin*dIII (for pEP104), and cloned into pMV261.kan, pJSC77 or pMV306.kan digested with the same enzymes. To construct Ms-PatA R95K, the Stratagene QuikChange site-directed mutagenesis protocol was used. Recovered plasmids were sequenced to verify the R95K mutation. To C-terminally HA-tag Ms-PatA and Ms-PatA R95K, PCR was performed with primers containing the HA epitope-encoding sequence. The PCR products were cloned into pCR2.1 by TA cloning and subcloned into pMV306.kan.

**Resazurin assays.** *M. smegmatis* growth and viability were monitored using resazurin. Cultures were grown in M9 media with 0.5 % glucose, 0.2 % glycerol, 0.1 % tyloxapol to saturation and then subcultured into new media. At an $OD_{600}$ of 1, cells were washed twice in M9 0.1 % tyloxapol (no added carbon source) and diluted to $10^6$ c.f.u. $ml^{-1}$. Cells (100 μl) were added to 96-well plates containing media as indicated. After 24 h of growth at 37 °C, resazurin (12.5 μg $ml^{-1}$ final concentration; Sigma) was added and fluorescence with excitation at 530 nm and emission at 590 nm was monitored over time. Values at 10 h post-resazurin addition are reported following normalization to the fluorescence value of the wild-type strain in the same growth media. A Student's *t*-test was used to determine if datasets were statistically significantly different. Negative controls always included media with no cells and cells with no added carbon source.

**Western blotting.** Whole-cell lysates of *M. smegmatis* grown in Mueller–Hinton media were prepared by 2–3 passages in a French press. Unlysed cells were removed by centrifugation and protein concentration was determined with a BCA assay (Pierce). Whole-cell lysates were separated by SDS-PAGE. The acetylated lysine primary antibody (Cell Signalling) was used at a 1 : 2500 dilution and was incubated with either BSA or acetylated BSA (100 μg $ml^{-1}$ final concentration) for 1 h on ice before addition to membranes. IRDye 800CW goat anti-rabbit polyclonal antibody (LI-COR) was used as the secondary antibody at a 1 : 15 000 dilution. The HA antibody (Covance) was used at a 1 : 20 000 dilution with the IRDye 680L T goat anti-mouse secondary antibody (LI-COR) used at a 1 : 20 000 dilution. Western blot results were visualized with an Odyssey fluorescence imaging system (LI-COR). Quantification of band densitometry was performed using Image J software (W. S. Rasband, NIH, Bethesda, MD, USA, 1997–2012; http://imagej.nih.gov/ij/). As a control for protein loading, a polyclonal SigA antibody (a kind gift from Murty Madiraju, The University of Texas Health Science Center, Tyler, TX, USA) was used at 1 : 20 000.

**In-gel trypsin digestion for MS analysis.** For both the wild-type and ΔdeAc mutant, 7 mg whole-cell lysate protein was separated on a 10 % SDS-PAGE gel (Bio-Rad). The protein bands were visualized by Coomassie blue R-250 staining (Bio-Rad), and gel slices corresponding to proteins 60–75 kDa in size were excised. Digestion of the excised gel slices was performed using 20 μg sequencing grade trypsin $ml^{-1}$ in 25 mM ammonium bicarbonate as described elsewhere (Collins *et al.*, 2008).

**Liquid chromatography (LC)-MS-MS.** Identification of proteins was done using reversed-phase LC-MS-MS analysis on a 2D-nanoLC Ultra system (Eksigent) coupled to an LTQ-Orbitrap Velos mass spectrometer (Thermo Scientific). The Eksigent system was configured to trap and elute peptides via a sandwiched injection of ~250 fmol sample. The trapping was performed on a 3 cm long,

**Table 1.** Bacterial strain list

| Strain | Description | Source |
|---|---|---|
| $mc^2155$ | Wild-type *M. smegmatis* | Snapper *et al.* (1990) |
| JDH032 | $mc^2155$ Δ*ms-acs* (*ms6179*) | This study |
| JDH008 | $mc^2155$ Δ*ms-srtN* (*ms5175*) | This study |
| JDH015 | $mc^2155$ Δ*ms4620* | This study |
| JDH037 | $mc^2155$ Δ*ms0171* | This study |
| JDH043 | $mc^2155$ Δ*ms-srtN* Δ*ms4620* Δ*ms0171* | This study |
| JDH050 | $mc^2155$ Δ*ms-patA* | This study |
| JDH051 | $mc^2155$ Δ*ms-srtN* Δ*ms4620* Δ*ms0171* Δ*ms-patA* | This study |

**Table 2.** Plasmids used in this study

| Plasmid | Description | Antibiotic marker | Source |
|---|---|---|---|
| pMV261.kan | Mycobacterial multicopy vector; *hsp60*-dependent promoter | $Kan^R$ | Stover *et al.* (1991) |
| pMV306.kan | Mycobacterial integrating vector | $Kan^R$ | Stover *et al.* (1991) |
| pJSC77 | HA-tag cloned into pMV261.kan | $Kan^R$ | Glickman *et al.* (2000) |
| pJV53 | Multicopy plasmid encoding phage Che9c *60* and *61* genes under acetamide-inducible promoter | $Kan^R$ | van Kessel & Hatfull (2008); van Kessel *et al.* (2008) |
| pMP614 | res-Hyg-res plasmid for constructing allelic exchange vectors | $Hyg^R$ | Kind gift from Martin Pavelka |
| pMP854 | *tnpR* expressing plasmid used to remove HygR marker from mutant strains | $Kan^R$ | Kind gift from Martin Pavelka |
| pJH33 | *M. smegmatis ms-acs* (*ms6179*) cloned into pMV261 | $Kan^R$ | This study |
| pEP104 | *M. tuberculosis mt-srtN* (*rv1151c*) cloned into pJSC77 | $Kan^R$ | This study |
| pJH40 | *M. smegmatis ms-patA* (*ms5458*) cloned into pMV306.kan | $Kan^R$ | This study |
| pJH51 | *M. smegmatis ms-patA* (*ms5458*) HA-tagged and cloned into pMV306.kan | $Kan^R$ | This study |
| pJH52 | *M. smegmatis ms-patA R95K* HA-tagged and cloned into pMV306.kan | $Kan^R$ | This study |

100 μm i.d. C18 column, while elution was performed on a 15 cm long, 75 μm i.d., 5 m, 300 Å particle ProteoPep II integraFrit C18 column (New Objective). Analytical separation of the tryptic peptides was achieved with a 120 min linear gradient of 2–10 % buffer B at 200 nl $min^{-1}$, where buffer A was an aqueous solution of 0.1 % formic acid and buffer B was a solution of 0.1 % formic acid in acetonitrile.

Mass spectrometric data acquisition was performed in a data-dependent manner via high-energy collision dissociation of the top 10 most abundant ions a hybrid LTQ-Orbitrap. Velos mass spectrometer mass spectra were processed, and peptide identification was performed using the Andromeda search engine found in MaxQuant software version 2.2.1 (Max Planck Institute, Germany). All protein database searches were performed against the *M. smegmatis* protein sequence database downloaded from PATRIC (Pathosystems Resource Integration Center) (http://patricbrc.org; Virginia Bioinformatics Institute, Blacksburg, VA, USA) (Gillespie *et al.*, 2011).

It should be noted that the PATRIC annotation for Ms-Acs (VBIMycSme59918_6019) differs from the National Center for Biotechnology Information annotation (YP_890399.1) and was used as a reference in this study because the molecular mass of Ms-Acs observed on our Western blots corresponds with the PATRIC annotation.

Peptides were identified using a target-decoy approach with a false discovery rate (FDR) of 1 % (Bantscheff *et al.*, 2012). A precursor ion mass tolerance of 100 p.p.m. was used for the first search that allowed for *m*/*z* retention time recalibration of precursor ions that were then subjected to a main search using a precursor ion mass tolerance of 5 p.p.m. and a product ion mass tolerance 0.5 Da. Search parameters included up to two missed cleavages at KR on the sequence (Cox & Mann, 2011), and lysine acetylation and methionine oxidation as dynamic PTMs. All acetylations representing a differential modification of 42.037 Da on lysines were unambiguously localized to specific residues using the built-in PTM score with a probability of >0.99.

**Acetyl peptide and protein quantification.** Label-free quantification was based on peak area (Bondarenko *et al.*, 2002; Chelius & Bondarenko, 2002; Gunawardena *et al.*, 2011). The measured area under the curve (AUC) of *m*/*z* and retention time aligned extracted ion chromatogram (XIC) of a peptide was performed via the label-free quantification module found in MaxQuant (version 1.2.2.5). Protein level quantification was performed using unique and razor peptide features corresponding to identifications filtered with a peptide FDR of 1 %, and protein FDR of 5 % and PTM FDR 1 %. Data processing was performed using Peseus (version 1.2.0.17) (Max Planck Institute, Germany) where relative quantification changes between samples were reported as fold-change differences. MaxQuant acetylated peptide-level quantification values were verified manually by integrating the AUC of the XIC using the Genesis peak detection and integration algorithm found in Xcalibure software (Thermo Scientific).

## RESULTS

### Acs is required for acetate metabolism in *M. smegmatis*

In other bacteria, Acs is required for growth on low levels of acetate as a sole carbon source and acetylation negatively regulates this activity (Castaño-Cerezo *et al.*, 2011; Gardner & Escalante-Semerena, 2009; Kumari *et al.*, 1995; Starai *et al.*, 2003). Before investigating the impact of lysine acetylation on Acs in mycobacteria, we first needed to establish a role for Ms-Acs in enabling growth of *M. smegmatis* on low levels of acetate. As there are no prior reports of Δ*acs* mutants of mycobacteria, we began by constructing an *M. smegmatis* mutant with a deletion of the annotated *ms-acs* gene (*ms6179*). Wild-type and the Δ*ms-acs* mutant were grown in M9 minimal media containing either glucose and glycerol or acetate for carbon sources. At various time points, culture aliquots were serially diluted and plated on glucose and glycerol containing agar to determine the number of c.f.u. Although the c.f.u. $ml^{-1}$ of the Δ*ms-acs* mutant was comparable to wild-type in glucose and glycerol media over time, the mutant exhibited a growth defect in media with acetate as the sole carbon source (Fig. 2a, b). The acetate growth phenotype of the Δ*ms-acs* mutant was complemented when the *M. smegmatis ms-acs* gene was expressed from a plasmid, which confirmed that this phenotype is due to the loss of Ms-Acs.

As another way to test for an acetate metabolism defect we employed a resazurin reduction assay (McNerney *et al.*,

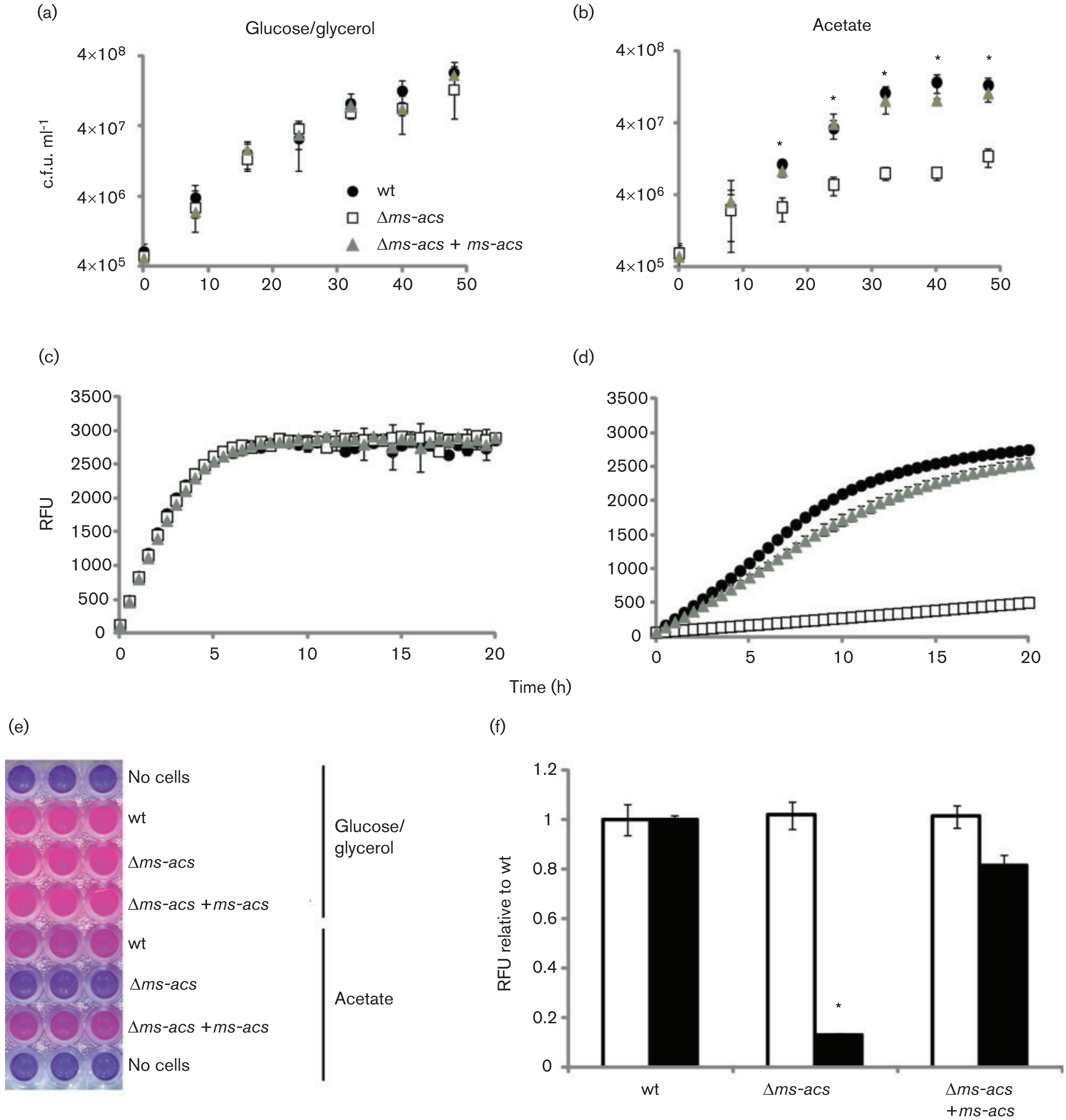


**Fig. 2.** Ms-Acs is required for acetate metabolism in *M. smegmatis*. (a) Growth curve of wild-type (mc$^2$155, pMV261), Δ*ms-acs* (JDH032, pMV261) and Δ*ms-acs* complemented with *ms-acs* (JDH032, pJH33) strains in glucose/glycerol media. Aliquots from liquid cultures were removed at the indicated time points and plated to enumerate c.f.u. ml$^{-1}$. (b) Growth curve of wild-type, Δ*ms-acs* and Δ*ms-acs* complemented with *ms-acs* strains in acetate media. Experiment is as described in (a). **P* value of <0.01 when comparing the wild-type and *ms-acs* strains. (c) Resazurin reduction in glucose/glycerol media. Liquid cultures of wild-type, Δ*ms-acs* and Δ*ms-acs* complemented with *ms-acs* strains were grown in 96-well plates as described in Methods. After 24 h, resazurin was added and relative fluorescence units (RFU) were measured over the next 20 h. (d) Resazurin reduction in acetate media, as described for (c). (e) The 96-well plate 10 h after resazurin was added. Pink colour indicates metabolically active cells, while blue shows low resazurin reduction and low metabolic activity. (f) Quantification of resazurin fluorescence for cells grown in glucose/glycerol (white bars) and acetate (black bars). The fluorescence value at 10 h after resazurin addition was normalized to that of the wild-type in each growth condition. **P* value of <0.01 when compared to wild-type fluorescence in the same media. For (a–d) and (f), error bars denote the SD of three replicates.

2000; Singh *et al.*, 2006). Resazurin is a blue compound that is reduced by metabolically active cells. When reduced, resazurin is converted to a pink fluorescent product that can be quantified to report on metabolic activity and cell number. Strains were grown in a 96-well plate in either glucose and glycerol or acetate-containing media. After 24 h incubation, resazurin was added and 10 h later visually inspected. In glucose and glycerol media, the wild-type, Δ*ms-acs* mutant and complemented *ms-acs* strain all showed robust resazurin reduction, as indicated by the pink colour (Fig. 2e). In acetate media, the wild-type and complemented strain also reduced resazurin, although the pink colour was not as strong as when the same strains were grown with glucose and glycerol, which are known to be better carbon sources. However, wells containing the Δ*ms-acs* mutant in acetate media maintained a blue colour, indicating reduced metabolic activity for the mutant (Fig. 2e). We also measured resazurin fluorescence over the course of 20 h (Fig. 2c, d). All strains converted resazurin at an equal rate in glucose and glycerol media. In acetate media, the wild-type and complemented strain reduced resazurin while the Δ*ms-acs* mutant showed very little to no resazurin reduction. In fact, the resazurin reduction of the Δ*ms-acs* mutant in acetate was comparable to what is seen when *M. smegmatis* is incubated with no carbon source (data not shown). For simplicity, we decided to report these data at a single time point of 10 h post-resazurin addition with the fluorescence value of each strain set relative to that of wild-type in the same carbon source (Fig. 2f). Taken together, the c.f.u. plating and resazurin assays demonstrated that, like in other bacteria, Ms-Acs is required for acetate metabolism and growth in acetate media.

## SrtN deacetylase regulates acetate metabolism in *M. smegmatis*

Having established function for Ms-Acs, we tested whether Ms-Acs and acetate metabolism are regulated by reversible lysine acetylation (Fig. 1a). If Ms-Acs is inhibited by lysine acetylation, there must exist at least one deacetylase that removes the acetyl group to activate Ms-Acs. Inspection of the *M. smegmatis* genome revealed three potential deacetylases. Ms-SrtN (Ms5175) and Ms4620 have homology to the class III, or sirtuin, family of deacetylases. They contain sirtuin consensus sequences and share amino acid similarity with the bacterial sirtuins CobB of *S. enterica* and SrtN of *B. subtilis* (Fig. 1b and Fig. S1). Ms-SrtN from *M. smegmatis* is the orthologue of Mt-SrtN from *M. tuberculosis*, with the two proteins sharing 81 % amino acid similarity. Ms4620 has no obvious *M. tuberculosis* orthologue. Ms0171 is a potential class I Zn-dependent deacetylase that is similar to the class I deacetylase AcuC of *B. subtilis* (Gardner & Escalante-Semerena, 2009) (Fig. 1b). There is no evident *M. tuberculosis* orthologue of Ms0171.

To identify the deacetylase(s) that acts on acetylated Ms-Acs in *M. smegmatis*, we deleted the genes encoding the three deacetylases individually and in combination. We predicted that in the absence of the responsible deacetylase, Ms-Acs would become locked in an acetylated (inactive) state resulting in an inability of *M. smegmatis* to utilize acetate as the sole carbon source. A Δ*ms-srtN* mutant behaved like wild-type *M. smegmatis* when grown in glucose and glycerol media, as measured by resazurin reduction (Fig. 3, white bars). However, in acetate media the Δ*ms-srtN* mutant exhibited significantly reduced metabolic activity, which is consistent with a function of Ms-SrtN in deacetylating Ms-Acs (Fig. 3, black bars). The acetate phenotype of the Δ*ms-srtN* mutant was complemented by providing a copy of the *M. tuberculosis srtN (mt-srtN)* gene. Together, these experiments demonstrated that Ms-SrtN is required for *M. smegmatis* to optimally metabolize acetate and further showed that Mt-SrtN of *M. tuberculosis* can also carry out this function. The Δ*ms-srtN* mutant phenotype was statistically significant compared to wild-type; however, it is noteworthy that this phenotype was not as severe as that of the Δ*ms-acs* mutant.

We also tested deletion mutants lacking *ms4620* or *ms0171*. Both of these mutants behaved like wild-type in glucose and glycerol media as well as in acetate media, indicating that on their own neither of these proteins is required for Acs deacetylation (Fig. 3). It remained a possibility, however, that the proteins have redundant deacetylase functions. To address this possibility, we constructed an unmarked mutant lacking all three *M. smegmatis* deacetylases, Δ*ms-srtN* Δ*ms4620* Δ*ms0171*. We refer to this triple deacetylase mutant as ΔdeAc. The ΔdeAc mutant exhibited a phenotype similar to the single Δ*ms-srtN* mutant when grown in acetate. Once again, introduction of the *mt-srtN* gene was sufficient to restore acetate metabolism to the ΔdeAc mutant. These results are consistent with negative regulation of Ms-Acs by lysine acetylation and with the function of Ms-SrtN and Mt-SrtN being to deacetylate mycobacterial Acs and enable acetate metabolism.

## PatA acetyltransferase regulates acetate metabolism in *M. smegmatis*

The *M. smegmatis* PatA (Ms5458, Ms-PatA) has been shown to acetylate Mt-Acs *in vitro* (Nambi *et al.*, 2010; Xu *et al.*, 2011). However, the *in vitro* studies did not test any of the 24 other putative GNATs in *M. smegmatis* that could possibly act on Ms-Acs (UniProt Consortium, 2012). To determine if Ms-PatA is the sole acetyltransferase that regulates Ms-Acs in *M. smegmatis*, we constructed Δ*ms-patA M. smegmatis* mutants in the wild-type and the ΔdeAc mutant background. In the model where lysine acetylation of Ms-Acs prevents the enzyme from converting acetate to acetyl-CoA, we predicted that a Δ*ms-patA* mutation in a wild-type strain would either enhance or have no effect on acetate metabolism. However, if Ms-PatA is the only acetyltransferase that acts on Ms-Acs then a *ms-patA* mutation should rescue the acetate phenotype of the ΔdeAc mutant. In other words, if Ms-Acs is not acetylated in the

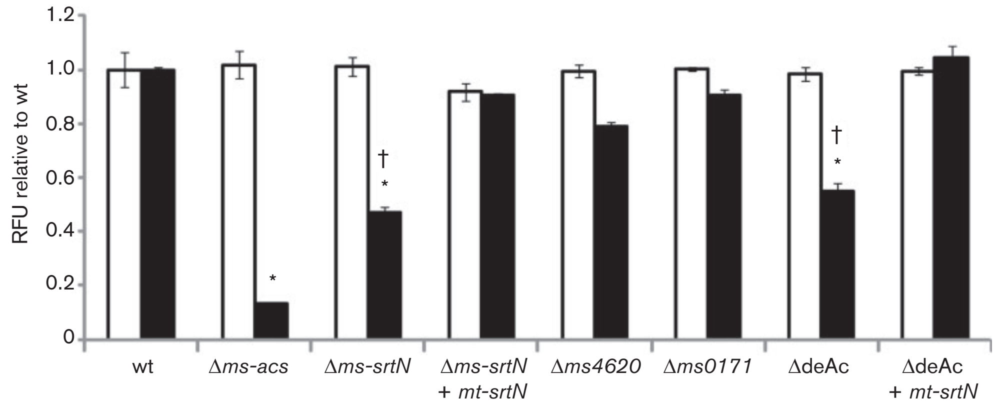


**Fig. 3.** Ms-SrtN is required for acetate metabolism in *M. smegmatis*. Resazurin reduction was fluorescently monitored and quantified as in Fig. 2(f). The strains included were wild-type (mc$^2$155, pMV261), Δ*ms-acs* (JDH032, pMV261), Δ*ms-srtN* (JDH008, pMV261), Δ*ms-srtN* complemented with *mt-srtN* (JDH008, pEP104), Δ*ms4620* (JDH015, pMV261), Δ*ms0171* (JDH037, pMV261), ΔdeAc (JDH043, pMV261), and ΔdeAc complemented with *mt-srtN* (JDH043, pEP104). White bars indicate cultures with glucose/glycerol and black bars indicate cultures with acetate as the sole carbon source. *$P<0.01$ when compared to wild-type fluorescence in the same media. †$P<0.01$ when compared to Δ*ms-acs* fluorescence in the same media.

first place, then the absence of the Ms-SrtN deacetylase should not impact acetate metabolism. Indeed, when the Δ*ms-patA* deletion was introduced into the triple deacetylase mutant, creating the quadruple mutant ΔdeAc Δ*ms-patA*, we found that it rescued the ΔdeAc acetate phenotype (Fig. 4). The effect of the Δ*ms-patA* deletion in the ΔdeAc mutant background could be complemented when *ms-patA* was provided on a plasmid, resulting in the return of an acetate metabolism defect. These results are consistent with Ms-PatA being the only acetyltransferase regulating Ms-Acs in *M. smegmatis*. The Δ*ms-patA* deletion in a wild-type background had no effect on *M. smegmatis* in glucose and glycerol media (Fig. 4). In acetate media the Δ*ms-patA* mutant consistently had slightly higher metabolic activity than wild-type, although this effect was not statistically significant.

Interestingly, the Ms-PatA complementation experiments revealed that Ms-PatA expression from a plasmid in the ΔdeAc mutant caused a more severe acetate phenotype than exhibited by the ΔdeAc mutant with Ms-PatA expressed from its native chromosomal location (compare the second and fourth black bars of Fig. 4). Although we have not quantified Ms-PatA levels, this difference could reflect higher expression off the complementing plasmid's *hsp60* promoter than from the chromosomal *ms-patA* locus.

## Ms-PatA activity requires cAMP binding in *M. smegmatis*

Mycobacterial Pat proteins are unique in that they contain an N-terminal cAMP-binding domain, and Ms-PatA requires cAMP for acetyltransferase activity *in vitro* (Nambi *et al.*, 2010; Xu *et al.*, 2011). In order to test if cAMP binding is also necessary for Ms-PatA activity in the context of the *M. smegmatis* cell, we tested a Ms-PatA protein in which the arginine at position 95, which is required for cAMP binding *in vitro*, was substituted with a lysine (Ms-PatA R95K) (Nambi *et al.*, 2010). Unlike the plasmid expressing Ms-PatA, when a plasmid expressing Ms-PatA R95K was introduced into the ΔdeAc Δ*ms-patA* strain, it failed to complement the Δ*ms-patA* mutation. The difference between the level of acetate metabolism of the ΔdeAc Δ*ms-patA* mutant expressing Ms-PatA compared to the strain expressing Ms-PatA R95K was statistically significant (Fig. 5a). To eliminate the possibility that the R95K substitution in Ms-PatA compromised protein stability, these experiments were performed with HA-tagged Ms-PatA and Ms-PatA R95K, and Western blotting confirmed equivalent levels of protein in the strains (Fig. 5b). These experiments validate the importance of cAMP binding to Ms-PatA, reported *in vitro* (Lee *et al.*, 2012; Nambi *et al.*, 2010; Xu *et al.*, 2011), to Ms-PatA function in the cellular context of intact *M. smegmatis*.

## Acetylated Ms-Acs is present in *M. smegmatis* whole-cell lysates

To examine Ms-Acs acetylation in cells more directly we used an antibody to acetylated lysine (Cell Signalling) and performed Western blotting of whole-cell lysates of *M. smegmatis* wild-type and the above-mentioned mutants (Fig. 6a). In wild-type *M. smegmatis*, a band close to the predicted molecular mass of Ms-Acs (69 kDa) was recognized by the acetylated lysine antibody. This band was absent in the Δ*ms-acs* mutant, but was present when a plasmid expressing Ms-Acs was introduced into the

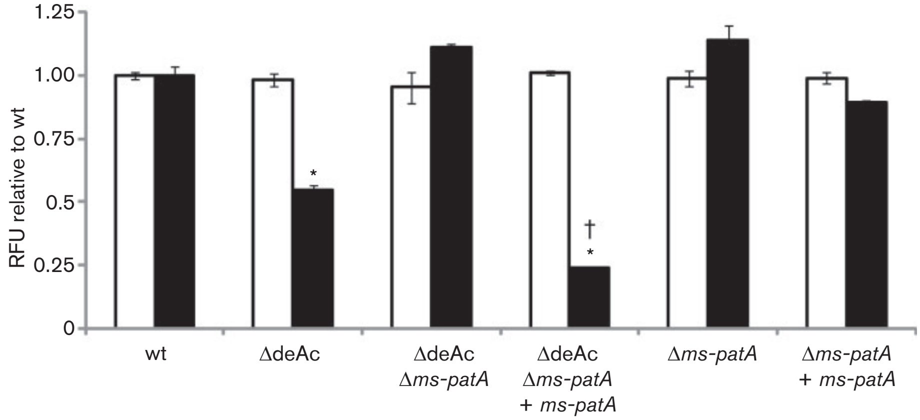


**Fig. 4.** Ms-PatA regulates acetate metabolism in *M. smegmatis*. Resazurin reduction was fluorescently monitored and quantified as in Fig. 2(f). The strains included were wild-type (mc$^2$155, pMV261), ΔdeAc (JDH043, pMV261), ΔdeAc Δ*ms-patA* (JDH051, pMV261), ΔdeAc Δ*ms-patA* complemented with *ms-patA* (JDH051, pJH40), Δ*ms-patA* (JDH050, pMV261), and Δ*ms-patA* complemented with *ms-patA* (JDH050, pJH40). White bars indicate cultures with glucose/glycerol and black bars indicate cultures with acetate as the sole carbon source. *$P<0.01$ when compared to wild-type fluorescence in the same media. †$P<0.01$ when compared to ΔdeAc fluorescence in the same media.

mutant, which confirmed the identity of this species as Ms-Acs. To establish the specificity of the antibody for acetylated lysines, we repeated the Western blotting in the presence of acetylated BSA (Fig. 6b). Including acetylated BSA led to a significant decrease in the intensity of the Acs band, confirming that the antibody recognition of Ms-Acs reflects its acetylation. Western blotting in the presence of acetylated BSA also revealed an unidentified protein that was non-specifically recognized by the antibody (Fig. 6b, marked by the plus sign).

We next determined the effects of the deacetylase and *ms-patA* mutations on Ms-Acs acetylation. Based on the acetate phenotypes of the deacetylase mutants, which prevented acetate metabolism presumably as a result of trapping Ms-Acs in an acetylated state, we expected the Δ*ms-srtN* and ΔdeAc mutants to show increased levels of acetylated Ms-Acs. Indeed, in both the Δ*ms-srtN* and ΔdeAc mutant strains, an increase in the amount of acetylated Ms-Acs was observed compared to the wild-type strain (Fig. 6). We also evaluated complemented strains in

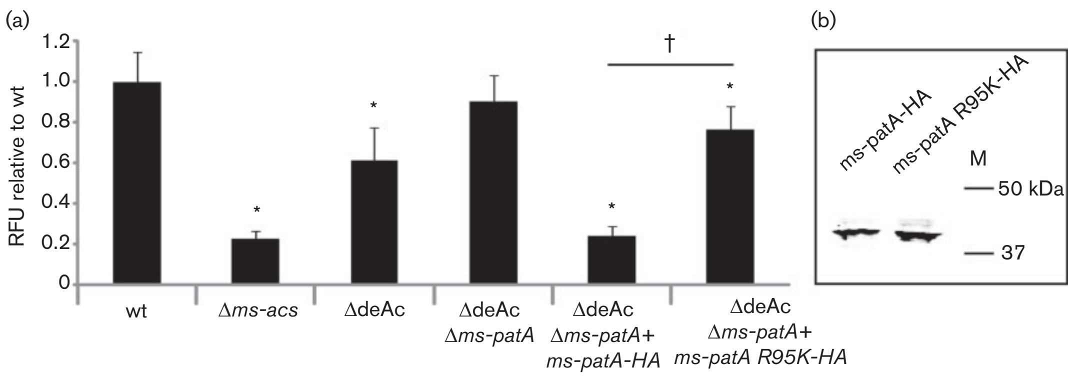


**Fig. 5.** cAMP binding is required for Ms-PatA activity in *M. smegmatis* cells. (a) Resazurin reduction for cultures grown with acetate as the sole carbon source was fluorescently monitored and quantified as in Fig. 2(f). The strains included were wild-type (mc$^2$155, pMV261), Δ*ms-acs* (JDH032, pMV261), ΔdeAc (JDH043, pMV261), ΔdeAc Δ*ms-patA* (JDH051, pMV261), ΔdeAc Δ*ms-patA* complemented with *ms-patA-HA* (JDH051, pJH51), and ΔdeAc Δ*ms-patA* complemented with *ms-patA R95K-HA* (JDH051, pJH52). *$P<0.01$ when compared to wild-type. †$P<0.01$ when comparing ΔdeAc Δ*ms-patA*+*ms-patA-HA* and ΔdeAc Δ*ms-patA*+*ms-patA R95K-HA*. (b) Western blot of whole-cell lysates of ΔdeAc Δ*ms-patA* complemented with *ms-patA-HA* (JDH051, pJH51) and ΔdeAc Δ*ms-patA* complemented with *ms-patA R95K-HA* (JDH051, pJH52) probed with anti-HA antibody. M, molecular mass marker.

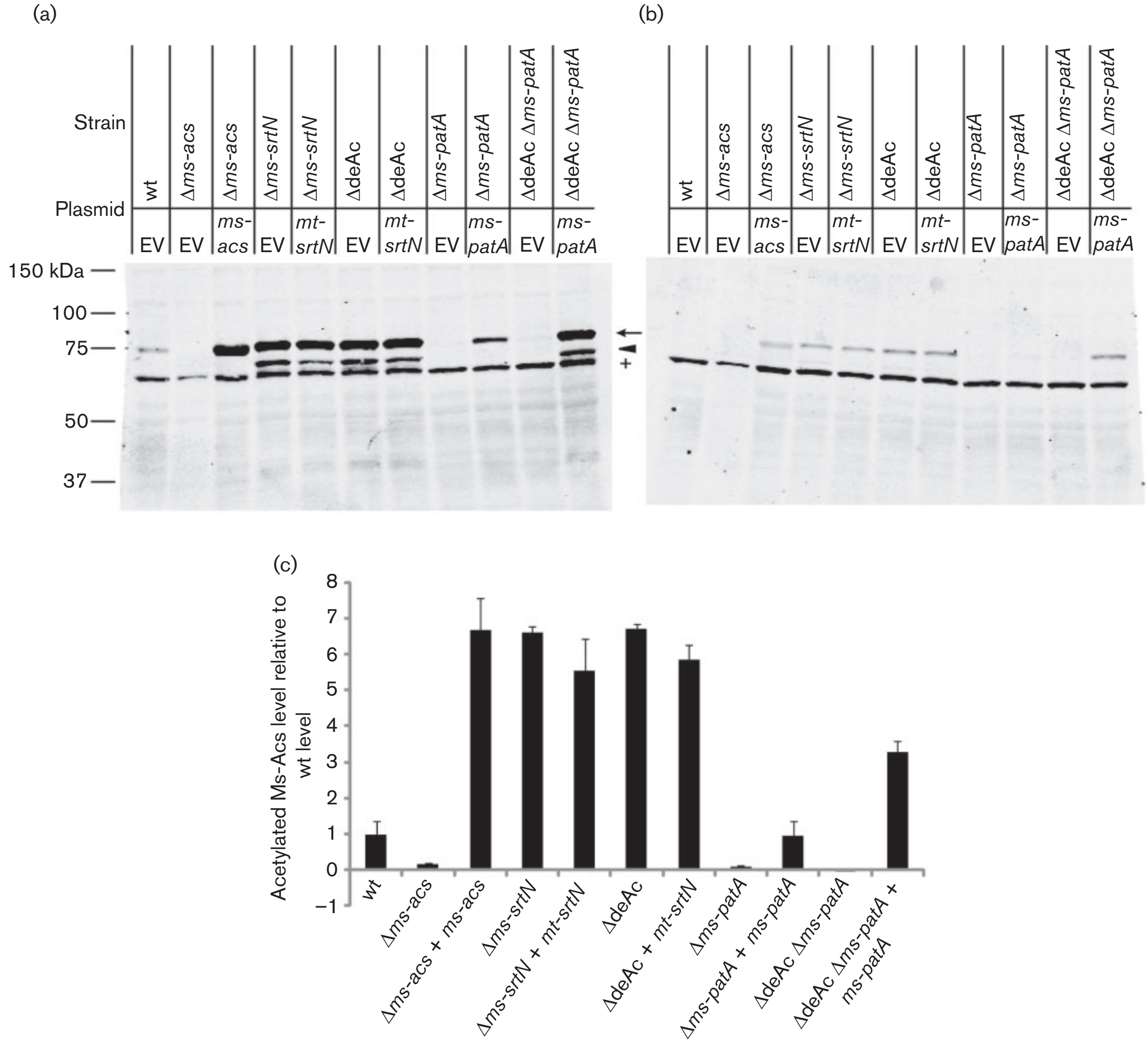


**Fig. 6.** Mycobacterial SrtN and PatA affect Ms-Acs acetylation. (a) Western blot of whole-cell lysates of indicated strains harbouring empty vectors (EV) or complementing plasmids (genes as indicated). Molecular mass marker band sizes are indicated on the left. The blot was probed with anti-acetyl-lysine antibody in the presence of BSA and shows all proteins detected by the antibody. The arrow points to the specific band corresponding to Ms-Acs, the plus sign indicates a non-specific band and the arrowhead indicates a specifically acetylated unknown protein. (b) Blot probed with anti-acetyl-lysine antibody in the presence of acetylated BSA. (c) Quantification of acetylated Ms-Acs in the strains from (a), performed in triplicate. Each sample was standardized by comparing to the amount of SigA (data not shown). Triplicate samples were then averaged and normalized to the levels of acetylated Ms-Acs in the wild-type strain.

which *mt-srtN* was introduced on a plasmid into the deacetylase mutant strains. Interestingly, in these *mt-srtN* complemented strains the level of acetylated Ms-Acs only decreased slightly, if at all (Fig. 6c). Because these *mt-srtN* complemented strains were able to metabolize acetate like wild-type (Fig. 3), this result suggested that the reduction in Ms-Acs acetylation needed for acetate metabolism is small.

Next we examined the levels of acetylated Ms-Acs in the Δ*ms-patA* strain. If Ms-PatA is the sole acetyltransferase that modifies Ms-Acs, there should be no acetylated Ms-Acs in the Δ*ms-patA* background. In fact, Western blotting revealed undetectable levels of acetylated Ms-Acs when *ms-patA* was deleted (Fig. 6). In complementing strains in which *ms-patA* was provided on an integrating plasmid, acetylated Ms-Acs was again detected. These data fit the model whereby, at least under the conditions tested, Ms-PatA is the sole acetyltransferase that acetylates Ms-Acs.

The Western blots also revealed another acetylated protein running at a slightly lower molecular mass (approx. 65 kDa) than Ms-Acs (Fig. 6a, marked by the arrowhead). This additional acetylated protein was not observed in all strains, but it was specifically detected in the deacetylase mutants (Δ*ms-srtN* and ΔdeAc) and in strains expressing *ms-patA* from a plasmid. Thus, this band appeared to correspond to another protein that can be acetylated by Ms-PatA and deacetylated by Ms-SrtN.

### Acetylated Ms-Acs and Ms5404 peptides are detected in *M. smegmatis* whole-cell lysates

To help identify the acetylated proteins revealed by Western blot, we employed quantitative MS. Whole cell lysates from the wild-type and ΔdeAc strains (two biological replicates of each) were separated by SDS-PAGE and gel slices spanning proteins approximately 60–75 kDa were excised, subjected to trypsin digestion and analysed by LC-MS-MS. Peptide sequences were identified using Andromeda (MaxQuant) and quantification was performed using label-free quantification to measure the AUC of the XIC of peptides (Cox *et al.*, 2011). The analysis unambiguously identified an acetylated Ms-Acs peptide, which was acetylated at lysine residue 589 in the peptide SGK(Ac)IMR (Fig. S2 available with the online version of this paper). This acetylated lysine in Ms-Acs corresponds to the site of acetylation in the *S. enterica* and *B. subtilis* Acs proteins. The acetylated Acs peptide was, as expected, more abundant (97.5-fold higher) in the ΔdeAc mutant compared to the wild-type strain (Table 3). In contrast, relatively equal levels of the Ms-Acs protein, quantified with at least five unique peptides, were identified in the ΔdeAc mutant and wild-type strains.

The 67kD Ms5404 protein was also identified as an acetylated protein by the MS analysis. Ms5404 is a predicted propionyl-CoA synthetase and the site of acetylation was unambiguously localized at lysine-586 in the identified peptide SGK(Ac)ILR (Fig S2). Notably, a propionyl-CoA synthetase from *S. enterica*, PrpE, is acetylated at the corresponding lysine (Garrity *et al.*, 2007). Interestingly, the acetylated Ms5404 peptide was only detected in the ΔdeAc samples while the relative levels of Ms5404 protein, quantified with at least five unique peptides, were similar in the ΔdeAc mutant and wild-type samples (Table 3). These results indicated that Ms5404 is another lysine acetylated protein of *M. smegmatis*. Its size of 67 kDa and our identification of acetylated peptides only in the ΔdeAc samples makes it a leading candidate for being the acetylated protein observed by Western blot in the ΔdeAc mutant, but not in wild-type (Fig. 6a).

### Ms-Acs, Ms-SrtN and Ms-PatA also regulate propionate metabolism

Our finding that another acetylated protein of *M. smegmatis* is Ms5404, a putative propionyl-CoA synthetase, along with the fact that propionate can be a substrate for Mt-Acs *in vitro* (Li *et al.*, 2011a), suggested that propionate metabolism in *M. smegmatis* may also be regulated by lysine acetylation. Therefore, we went on to evaluate the deacetylase and acetyltransferase mutants in media with propionate as the sole carbon source. The Δ*ms-srtN* and ΔdeAc mutants had reduced metabolic activity when propionate was the sole carbon source (Fig. 7). Similar to what was seen with acetate, addition of the Δ*ms-patA* mutation into the ΔdeAc background rescued propionate metabolism. All the propionate phenotypes were complemented when the appropriate genes were provided on a plasmid. These results indicated that Ms-SrtN and Ms-PatA additionally regulate propionate metabolism in *M. smegmatis*. While the Δ*ms-acs* mutant also had a phenotype, the metabolism defect of the mutant in propionate was not as complete as seen in acetate (compare Fig. 3 and Fig. 7), suggesting there could be another protein acting as a propionyl-CoA synthetase in the cell, with Ms5404 being a leading candidate.

## DISCUSSION

In comparison to eukaryotic cells, lysine acetylation in bacteria is a more recently recognized phenomenon that has so far only been studied in a small number of bacterial species. Acs is the best-studied example of a bacterial protein regulated by lysine acetylation, and previous *in vitro* studies demonstrate the ability of mycobacterial Pat and SrtN enzymes to acetylate and deacetylate purified Acs, respectively (Gu *et al.*, 2009; Li *et al.*, 2011a; Xu *et al.*, 2011). Published work also shows that the Pat protein of *Mycobacterium bovis* BCG is necessary for growth on

**Table 3.** Label-free quantification values obtained for Ms-Acs and Ms5404 proteins and their detectable acetylated peptides

| | Label-free AUC | | | | Mean fold change (ΔdeAc/wt) |
|---|---|---|---|---|---|
| | wt-1 | wt-2 | ΔdeAc-1 | ΔdeAc-2 | |
| **Ms-Acs protein** | $2.2\times10^{8}$ | $1.1\times10^{8}$ | $6.4\times10^{8}$ | $5.1\times10^{7}$ | 2.1 |
| **Ms-Acs SGK(Ac)IMR** | $1.3\times10^{7}$ | ND | $5.5\times10^{8}$ | $7.5\times10^{8}$ | 97.5 |
| **Ms5404 protein** | $5.6\times10^{6}$ | $2.1\times10^{6}$ | $3.6\times10^{6}$ | $5.0\times10^{6}$ | 1.1 |
| **Ms5404 SGK(Ac)ILR** | ND | ND | $1.1\times10^{5}$ | $2.0\times10^{6}$ | 1030.7 |

ND, peptides that had no detectable XIC-AUC in label-free quantification, but were assigned a value equal to a base line noise level of $1.0\times10^{3}$ in order to calculate a fold-change value.

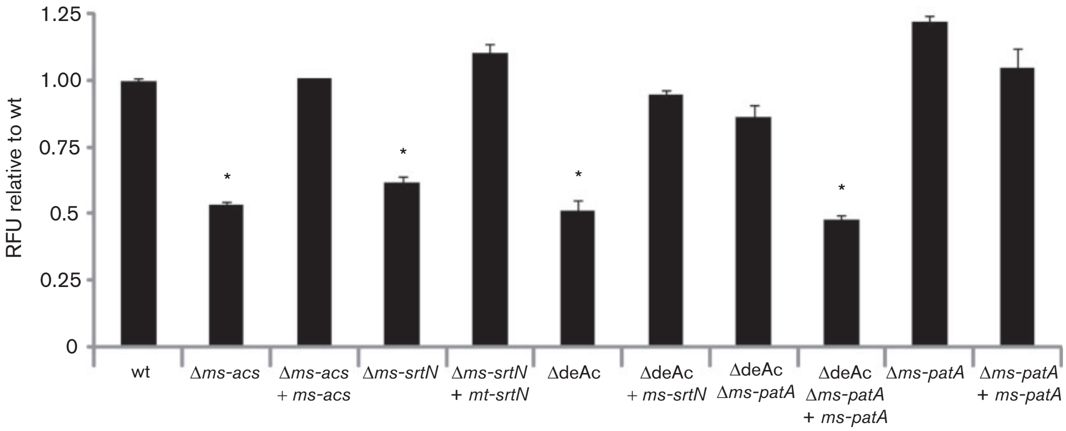


**Fig. 7.** Propionate metabolism is regulated by Ms-Acs, Ms-SrtN and Ms-PatA in *M. smegmatis*. Resazurin reduction of cells growing with propionate as the sole carbon source was fluorescently monitored and quantified as in Fig. 2(f). The strains included were wild-type (mc$^2$155, pMV261), Δ*ms-acs* (JDH032, pMV261), Δ*ms-acs* complemented with *ms-acs* (JDH032, pJH33), Δ*ms-srtN* (JDH008, pMV261), Δ*ms-srtN* complemented with *mt-srtN* (JDH008, pEP104), ΔdeAc (JDH043, pMV261), ΔdeAc complemented with *mt-srtN* (JDH043, pEP104), ΔdeAc Δ*ms-patA* (JDH051, pMV261), ΔdeAc Δ*ms-patA* complemented with *ms-patA* (JDH051, pJH40), Δ*ms-patA* (JDH050, pMV261), and Δ*ms-patA* complemented with *ms-patA* (JDH050, pJH40). *$P < 0.01$ when compared to wild-type fluorescence in the same media.

propionate as a sole carbon source (Nambi *et al.*, 2013). However, none of the past studies demonstrated the biological significance of the Acs acetylation/deacetylation regulatory circuit on acetate metabolism in mycobacteria. In the present study, we demonstrated a role for the lysine acetyltransferase Ms-PatA and deacetylase Ms-SrtN in regulating Ms-Acs and acetate metabolism in the context of the cell. Thus, the results reported here are significant in providing critical validation of the data obtained by *in vitro* studies with purified proteins. We also confirmed that the cAMP binding of Ms-PatA is important for its function and we identified an additional example of an acetylated protein, Ms5404, in *M. smegmatis*.

## Specificity of Ms-SrtN and Ms-PatA enzymes

There are several putative lysine acetyltransferases and deacetylases encoded by the *M. smegmatis* genome. It was a strong possibility that acetylation in mycobacteria would involve multiple modifying enzymes and prove more complicated than observed *in vitro*. In fact, in *B. subtilis*, two deacetylases are required for Acs deacetylation and growth on acetate (Gardner & Escalante-Semerena, 2009). However, we found only one deacetylase, Ms-SrtN, acted on acetylated Ms-Acs. Ms-SrtN is the orthologue of the sole predicted deacetylase in *M. tuberculosis*, Mt-SrtN. When complementing the Δ*ms-srtN* mutant phenotype we used a plasmid expressing Mt-SrtN, which demonstrated conservation of function of the *M. tuberculosis* and *M. smegmatis* SrtN proteins. The functions of the other two putative *M. smegmatis* deacetylases are still in question. While there was no evidence for either Ms4620 or Ms0171 acting on Ms-Acs, they may deacetylate other substrates. Given the large number of putative GNAT-type acetyltransferases (UniProt Consortium, 2012), we also thought it possible that more than one of these proteins would act on Ms-Acs, but that was not the case. Thus, there appears to be a high level of substrate specificity for the Ms-SrtN and Ms-PatA pair.

Data in this study are believed to be the first to show an acetate phenotype for mycobacterial deacetylase mutants. The acetate phenotypes of the deacetylase mutants (Δ*ms-srtN* or ΔdeAc) were reproducible, complementable and statistically significant, but they were not as severe as the phenotype of the Δ*ms-acs* mutant. In fact, until we turned to the resazurin assay to measure acetate metabolism it was difficult to observe a phenotype, which may be why there were no earlier reports of deacetylation regulating acetate metabolism in intact cells. The more moderate phenotype of the deacetylase mutants suggested that there still existed some active unacetylated Ms-Acs in these strains. This could be due to the presence of an unidentified deacetylase. However, we think it more likely that the ΔdeAc acetate phenotype is due to newly synthesized Ms-Acs that had yet to be acetylated in the cell, possibly as a consequence of limited amount or acetylation efficiency of Ms-PatA. Support for this idea comes from experiments where the acetate defect of the ΔdeAc mutant was enhanced by providing an exogenous copy of Ms-PatA on a single copy vector (Fig. 4, compare ΔdeAc and ΔdeAc Δ*ms-patA* + *ms-patA*). In addition, overexpressing Ms-PatA from a multi-copy vector in a wild-type background prevented *M. smegmatis* growth on acetate (data not shown). These experiments suggested that the level of Ms-PatA influences the amount of acetylated inactive Ms-Acs in the cell.

### An additional metabolic process regulated by Ms-Acs, Ms-SrtN and Ms-PatA

Our data also revealed a role for Ms-Acs, Ms-SrtN and Ms-PatA in regulating propionate metabolism in *M. smegmatis* (Fig. 7). *In vitro* studies show Mt-Acs to be able to use propionate, in addition to acetate, to generate CoA derivatives (Li *et al.*, 2011a; Xu *et al.*, 2011). However, it is likely that Ms-Acs is not the sole propionyl-CoA synthetase in *M. smegmatis* because the Δ*ms-acs* phenotype in propionate was not complete. The other protein we identified by MS as being lysine acetylated, Ms5404, is the leading candidate for being an additional propionyl-CoA synthetase that could enable propionate utilization by *M. smegmatis*. In *S. enterica*, both Acs and a protein called PrpE have propionyl-CoA synthetase activity but, in this case, both proteins need to be absent in order to observe a phenotype on propionate (Horswill & Escalante-Semerena, 1999).

In our study the Δ*ms-patA* mutation in a wild-type background did not exhibit a defect in propionate metabolism, although it did rescue the ΔdeAc phenotype. This differs from the recent report of an *M. bovis* BCG Δ*pat* mutant (Δ*KATbcg*) being defective for growth in propionate (Nambi *et al.*, 2013). The BCG Δ*pat* mutant phenotype was interpreted as resulting from a build-up of Acs-generated toxic propionyl-CoA metabolites. Interestingly, in this study, it was also shown that the BCG Acs can be propionylated by PatA and depropionylated by SrtN *in vitro* (Nambi *et al.*, 2013), suggesting that acetylation and propionylation may provide overlapping levels of regulation in mycobacteria. Because propionyl-CoA metabolite accumulation can also be toxic to *M. smegmatis* (Upton & McKinney, 2007), the different results we obtained with the Δ*ms-patA* mutant may be accounted for by differences in experimental conditions and/or the specific metabolic pathways operating in each species to prevent propionyl-CoA build-up (Rhee *et al.*, 2011). It also remains possible that the phenotype of the BCG Δ*patA* mutant reflects PatA regulated proteins other than Acs since the phenotype of a BCG Δ*acs* mutant in propionate is unknown. Nonetheless, from the studies of Δ*patA* mutants in *M. smegmatis* and BCG it is evident that propionate metabolism in mycobacteria is regulated by PatA.

### Expanding our understanding of mycobacterial metabolic regulation

Until recently, the only mode of metabolic regulation reported in mycobacteria was transcriptional regulation of metabolic genes (Datta *et al.*, 2011; Schnappinger *et al.*, 2003; Timm *et al.*, 2003). Interestingly, both the mycobacterial SrtN and PatA enzymes themselves are regulated by different cellular signals. Transcript levels of the *patA* gene of *M. bovis* BCG are reported to be regulated by propionate and SDS (Nambi *et al.*, 2013). In addition, cAMP binding to Mt-PatA causes major conformational changes (Lee *et al.*, 2012) and increases the acetylation activity of both Ms-PatA and Mt-PatA proteins *in vitro* (Nambi *et al.*, 2010; Xu *et al.*, 2011). Our data extend these *in vitro* results in showing that cAMP binding is also necessary for PatA activity in *M. smegmatis* cells. In *M. tuberculosis*, cAMP levels are regulated by several conditions associated with infection (Bai *et al.*, 2011). Interestingly, cAMP also regulates the PatZ lysine acetyltransferase of *E. coli*, but it does so by a different mechanism involving transcriptional regulation (Castaño-Cerezo *et al.*, 2011).

On the deacetylase side of the equation, the mycobacterial sirtuin deacetylases Ms-SrtN and Mt-SrtN are shown to be $NAD^+$-dependent deacetylases *in vitro* (Gu *et al.*, 2009; Nambi *et al.*, 2013; Xu *et al.*, 2011). $NAD^+$ levels reflect the energy status of the cell. In addition to cAMP and $NAD^+$, the level of acetyl-CoA, which is used in the acetylation reaction and is another reflection of the carbon and energy status of the cell, will also influence the amount of acetylation that occurs. Consequently, reversible acetylation by the mycobacterial PatA and SrtN pair provides an interesting example of how multiple signals and regulatory networks can be integrated to achieve metabolic regulation.

There are likely to be many mycobacterial proteins regulated by lysine acetylation besides Ms-Acs and Ms5404. In other studies, a universal stress protein, Ms4207, of *M. smegmatis* was reported to be acetylated by Ms-PatA (Nambi *et al.*, 2010) and FadD13 was identified as acetylated in *M. bovis* BCG cells (Nambi *et al.*, 2013). However, the biological significance of Ms4207 or FadD13 acetylation has yet to be shown. There are also multiple FadD proteins (fatty acyl-CoA ligases) from *M. tuberculosis* shown to be acetylated and deacetylated by PatA and SrtN with purified proteins *in vitro* (Nambi *et al.*, 2013). There is additionally a report of a Δ*ms-srtN* mutant having a defect in DNA double strand break repair, although this phenotype has not been linked to deacetylation of any substrates (Li *et al.*, 2011b). In the future it will be important to identify the full acetylome of mycobacterium species, especially *M. tuberculosis*.

Reversible acetylation is a strong candidate for dynamically controlling metabolic pathways and enabling *M. tuberculosis* to quickly adapt to the changing host environment. By showing here that the regulatory circuit of Acs acetylation and deacetylation by PatA and SrtN enzymes holds true in *M. smegmatis*, this work opens the door to studying reversible acetylation and how it integrates regulatory signals in the cellular environment of mycobacteria.

## ACKNOWLEDGEMENTS

We thank Martin Pavelka for the kind gift of plasmids and Murty Madiraju for antibodies. We also thank members of the Braunstein Lab for helpful discussions and critical reading of the manuscript. This work was supported by NIH grant AI054540 awarded to M. B. L. R. B was supported by the UNC Postbaccalaureate Research Education Program (NIH grant 5R25GM089569).

## REFERENCES

**Bai, G., Knapp, G. S. & McDonough, K. A. (2011).** Cyclic AMP signalling in mycobacteria: redirecting the conversation with a common currency. *Cell Microbiol* **13**, 349–358.

**Bantscheff, M., Lemeer, S., Savitski, M. M. & Kuster, B. (2012).** Quantitative mass spectrometry in proteomics: critical review update from 2007 to the present. *Anal Bioanal Chem* **404**, 939–965.

**Barak, R., Welch, M., Yanovsky, A., Oosawa, K. & Eisenbach, M. (1992).** Acetyladenylate or its derivative acetylates the chemotaxis protein CheY in vitro and increases its activity at the flagellar switch. *Biochemistry* **31**, 10099–10107.

**Barak, R., Prasad, K., Shainskaya, A., Wolfe, A. J. & Eisenbach, M. (2004).** Acetylation of the chemotaxis response regulator CheY by acetyl-CoA synthetase purified from *Escherichia coli*. *J Mol Biol* **342**, 383–401.

**Bondarenko, P. V., Chelius, D. & Shaler, T. A. (2002).** Identification and relative quantitation of protein mixtures by enzymatic digestion followed by capillary reversed-phase liquid chromatography-tandem mass spectrometry. *Anal Chem* **74**, 4741–4749.

**Castaño-Cerezo, S., Bernal, V., Blanco-Catalá, J., Iborra, J. L. & Cánovas, M. (2011).** cAMP-CRP co-ordinates the expression of the protein acetylation pathway with central metabolism in *Escherichia coli*. *Mol Microbiol* **82**, 1110–1128.

**Chelius, D. & Bondarenko, P. V. (2002).** Quantitative profiling of proteins in complex mixtures using liquid chromatography and mass spectrometry. *J Proteome Res* **1**, 317–323.

**Collins, M. O., Yu, L. & Choudhary, J. S. (2008).** Analysis protein complexes by 1D-SDS-PAGE and tandem mass spectrometry. Protocol Exchange, http://www.nature.com/protocolexchange/protocols/455.

**Cox, J. & Mann, M. (2011).** Quantitative, high-resolution proteomics for data-driven systems biology. *Annu Rev Biochem* **80**, 273–299.

**Cox, J., Neuhauser, N., Michalski, A., Scheltema, R. A., Olsen, J. V. & Mann, M. (2011).** Andromeda: a peptide search engine integrated into the MaxQuant environment. *J Proteome Res* **10**, 1794–1805.

**Crosby, H. A., Heiniger, E. K., Harwood, C. S. & Escalante-Semerena, J. C. (2010).** Reversible N epsilon-lysine acetylation regulates the activity of acyl-CoA synthetases involved in anaerobic benzoate catabolism in *Rhodopseudomonas palustris*. *Mol Microbiol* **76**, 874–888.

**Datta, P., Shi, L., Bibi, N., Balázsi, G. & Gennaro, M. L. (2011).** Regulation of central metabolism genes of *Mycobacterium tuberculosis* by parallel feed-forward loops controlled by sigma factor E ($\sigma^E$). *J Bacteriol* **193**, 1154–1160.

**Eisenreich, W., Dandekar, T., Heesemann, J. & Goebel, W. (2010).** Carbon metabolism of intracellular bacterial pathogens and possible links to virulence. *Nat Rev Microbiol* **8**, 401–412.

**Gardner, J. G. & Escalante-Semerena, J. C. (2009).** In *Bacillus subtilis*, the sirtuin protein deacetylase, encoded by the *srtN* gene (formerly *yhdZ*), and functions encoded by the *acuABC* genes control the activity of acetyl coenzyme A synthetase. *J Bacteriol* **191**, 1749–1755.

**Gardner, J. G., Grundy, F. J., Henkin, T. M. & Escalante-Semerena, J. C. (2006).** Control of acetyl-coenzyme A synthetase (AcsA) activity by acetylation/deacetylation without NAD(+) involvement in *Bacillus subtilis*. *J Bacteriol* **188**, 5460–5468.

**Garrity, J., Gardner, J. G., Hawse, W., Wolberger, C. & Escalante-Semerena, J. C. (2007).** N-lysine propionylation controls the activity of propionyl-CoA synthetase. *J Biol Chem* **282**, 30239–30245.

**Gillespie, J. J., Wattam, A. R., Cammer, S. A., Gabbard, J. L., Shukla, M. P., Dalay, O., Driscoll, T., Hix, D., Mane, S. P. & other authors (2011).** PATRIC: the comprehensive bacterial bioinformatics resource with a focus on human pathogenic species. *Infect Immun* **79**, 4286–4298.

**Glickman, M. S., Cox, J. S. & Jacobs, W. R., Jr (2000).** A novel mycolic acid cyclopropane synthetase is required for cording, persistence, and virulence of *Mycobacterium tuberculosis*. *Mol Cell* **5**, 717–727.

**Gu, J., Deng, J. Y., Li, R., Wei, H., Zhang, Z., Zhou, Y., Zhang, Y. & Zhang, X. E. (2009).** Cloning and characterization of NAD-dependent protein deacetylase (Rv1151c) from *Mycobacterium tuberculosis*. *Biochemistry (Mosc)* **74**, 743–748.

**Gunawardena, H. P., Huang, Y., Kenjale, R., Wang, H., Xie, L. & Chen, X. (2011).** Unambiguous characterization of site-specific phosphorylation of leucine-rich repeat Fli-I-interacting protein 2 (LRRFIP2) in Toll-like receptor 4 (TLR4)-mediated signaling. *J Biol Chem* **286**, 10897–10910.

**Horswill, A. R. & Escalante-Semerena, J. C. (1999).** The *prpE* gene of *Salmonella typhimurium* LT2 encodes propionyl-CoA synthetase. *Microbiology* **145**, 1381–1388.

**Kim, D., Yu, B. J., Kim, J. A., Lee, Y. J., Choi, S. G., Kang, S. & Pan, J. G. (2013).** The acetylproteome of Gram-positive model bacterium *Bacillus subtilis*. *Proteomics* **13**, 1726–1736.

**Kumari, S., Tishel, R., Eisenbach, M. & Wolfe, A. J. (1995).** Cloning, characterization, and functional expression of acs, the gene which encodes acetyl coenzyme A synthetase in *Escherichia coli*. *J Bacteriol* **177**, 2878–2886.

**Lee, H. J., Lang, P. T., Fortune, S. M., Sassetti, C. M. & Alber, T. (2012).** Cyclic AMP regulation of protein lysine acetylation in *Mycobacterium tuberculosis*. *Nat Struct Mol Biol* **19**, 811–818.

**Li, R., Gu, J., Chen, P., Zhang, Z., Deng, J. & Zhang, X. (2011a).** Purification and characterization of the acetyl-CoA synthetase from *Mycobacterium tuberculosis*. *Acta Biochim Biophys Sin (Shanghai)* **43**, 891–899.

**Li, Z., Wen, J., Lin, Y., Wang, S., Xue, P., Zhang, Z., Zhou, Y., Wang, X., Sui, L. & other authors (2011b).** A Sir2-like protein participates in mycobacterial NHEJ. *PLoS ONE* **6**, e20045.

**Lima, B. P., Antelmann, H., Gronau, K., Chi, B. K., Becher, D., Brinsmade, S. R. & Wolfe, A. J. (2011).** Involvement of protein acetylation in glucose-induced transcription of a stress-responsive promoter. *Mol Microbiol* **81**, 1190–1204.

**Lima, B. P., Thanh Huyen, T. T., Bäsell, K., Becher, D., Antelmann, H. & Wolfe, A. J. (2012).** Inhibition of acetyl phosphate-dependent transcription by an acetylatable lysine on RNA polymerase. *J Biol Chem* **287**, 32147–32160.

**Marrero, J., Rhee, K. Y., Schnappinger, D., Pethe, K. & Ehrt, S. (2010).** Gluconeogenic carbon flow of tricarboxylic acid cycle intermediates is critical for *Mycobacterium tuberculosis* to establish and maintain infection. *Proc Natl Acad Sci U S A* **107**, 9819–9824.

**McKinney, J. D., Höner zu Bentrup, K., Muñoz-Elías, E. J., Miczak, A., Chen, B., Chan, W. T., Swenson, D., Sacchettini, J. C., Jacobs, W. R., Jr & Russell, D. G. (2000).** Persistence of *Mycobacterium tuberculosis* in macrophages and mice requires the glyoxylate shunt enzyme isocitrate lyase. *Nature* **406**, 735–738.

**McNerney, R., Kiepiela, P., Bishop, K. S., Nye, P. M. & Stoker, N. G. (2000).** Rapid screening of *Mycobacterium tuberculosis* for susceptibility to rifampicin and streptomycin. *Int J Tuberc Lung Dis* **4**, 69–75.

**Muñoz-Elías, E. J. & McKinney, J. D. (2005).** *Mycobacterium tuberculosis* isocitrate lyases 1 and 2 are jointly required for *in vivo* growth and virulence. *Nat Med* **11**, 638–644.

**Muñoz-Elías, E. J. & McKinney, J. D. (2006).** Carbon metabolism of intracellular bacteria. *Cell Microbiol* **8**, 10–22.

**Nambi, S., Basu, N. & Visweswariah, S. S. (2010).** cAMP-regulated protein lysine acetylases in mycobacteria. *J Biol Chem* **285**, 24313–24323.

**Nambi, S., Gupta, K., Bhattacharyya, M., Ramakrishnan, P., Ravikumar, V., Siddiqui, N., Thomas, A. T. & Visweswariah, S. S. (2013).** Cyclic AMP-dependent protein lysine acylation in mycobacteria regulates fatty acid and propionate metabolism. *J Biol Chem* **288**, 14114–14124.

**Ramakrishnan, R., Schuster, M. & Bourret, R. B. (1998).** Acetylation at Lys-92 enhances signaling by the chemotaxis response regulator protein CheY. *Proc Natl Acad Sci U S A* **95**, 4918–4923.

**Rhee, K. Y., de Carvalho, L. P. S., Bryk, R., Ehrt, S., Marrero, J., Park, S. W., Schnappinger, D., Venugopal, A. & Nathan, C. (2011).** Central carbon metabolism in *Mycobacterium tuberculosis*: an unexpected frontier. *Trends Microbiol* **19**, 307–314.

**Schnappinger, D., Ehrt, S., Voskuil, M. I., Liu, Y., Mangan, J. A., Monahan, I. M., Dolganov, G., Efron, B., Butcher, P. D. & other authors (2003).** Transcriptional adaptation of *Mycobacterium tuberculosis* within macrophages: insights into the phagosomal environment. *J Exp Med* **198**, 693–704.

**Singh, A., Mai, D., Kumar, A. & Steyn, A. J. (2006).** Dissecting virulence pathways of *Mycobacterium tuberculosis* through protein-protein association. *Proc Natl Acad Sci U S A* **103**, 11346–11351.

**Snapper, S. B., Melton, R. E., Mustafa, S., Kieser, T. & Jacobs, W. R., Jr (1990).** Isolation and characterization of efficient plasmid transformation mutants of *Mycobacterium smegmatis*. *Mol Microbiol* **4**, 1911–1919.

**Starai, V. J. & Escalante-Semerena, J. C. (2004).** Identification of the protein acetyltransferase (Pat) enzyme that acetylates acetyl-CoA synthetase in *Salmonella enterica*. *J Mol Biol* **340**, 1005–1012.

**Starai, V. J., Celic, I., Cole, R. N., Boeke, J. D. & Escalante-Semerena, J. C. (2002).** Sir2-dependent activation of acetyl-CoA synthetase by deacetylation of active lysine. *Science* **298**, 2390–2392.

**Starai, V. J., Takahashi, H., Boeke, J. D. & Escalante-Semerena, J. C. (2003).** Short-chain fatty acid activation by acyl-coenzyme A synthetases requires SIR2 protein function in *Salmonella enterica* and *Saccharomyces cerevisiae*. *Genetics* **163**, 545–555.

**Stover, C. K., de la Cruz, V. F., Fuerst, T. R., Burlein, J. E., Benson, L. A., Bennett, L. T., Bansal, G. P., Young, J. F., Lee, M. H. & other authors (1991).** New use of BCG for recombinant vaccines. *Nature* **351**, 456–460.

**Thao, S., Chen, C. S., Zhu, H. & Escalante-Semerena, J. C. (2010).** Nε-lysine acetylation of a bacterial transcription factor inhibits Its DNA-binding activity. *PLoS ONE* **5**, e15123.

**Timm, J., Post, F. A., Bekker, L. G., Walther, G. B., Wainwright, H. C., Manganelli, R., Chan, W. T., Tsenova, L., Gold, B. & other authors (2003).** Differential expression of iron-, carbon-, and oxygen-responsive mycobacterial genes in the lungs of chronically infected mice and tuberculosis patients. *Proc Natl Acad Sci U S A* **100**, 14321–14326.

**UniProt Consortium (2012).** Reorganizing the protein space at the Universal Protein Resource (UniProt). *Nucleic Acids Res* **40** (Database issue), D71–D75.

**Upton, A. M. & McKinney, J. D. (2007).** Role of the methylcitrate cycle in propionate metabolism and detoxification in *Mycobacterium smegmatis*. *Microbiology* **153**, 3973–3982.

**van Kessel, J. C. & Hatfull, G. F. (2008).** Mycobacterial recombineering. *Methods Mol Biol* **435**, 203–215.

**van Kessel, J. C., Marinelli, L. J. & Hatfull, G. F. (2008).** Recombineering mycobacteria and their phages. *Nat Rev Microbiol* **6**, 851–857.

**Wang, Q., Zhang, Y., Yang, C., Xiong, H., Lin, Y., Yao, J., Li, H., Xie, L., Zhao, W. & other authors (2010).** Acetylation of metabolic enzymes coordinates carbon source utilization and metabolic flux. *Science* **327**, 1004–1007.

**WHO (2013).** *Tuberculosis*; fact sheet no. 104, http://www.who.int/mediacentre/factsheets/fs104/en#global. Geneva: World Health Organization.

**Wu, X., Vellaichamy, A., Wang, D., Zamdborg, L., Kelleher, N. L., Huber, S. C. & Zhao, Y. (2013).** Differential lysine acetylation profiles of *Erwinia amylovora* strains revealed by proteomics. *J Proteomics* **79**, 60–71.

**Xu, H., Hegde, S. S. & Blanchard, J. S. (2011).** Reversible acetylation and inactivation of *Mycobacterium tuberculosis* acetyl-CoA synthetase is dependent on cAMP. *Biochemistry* **50**, 5883–5892.

**Yan, J., Barak, R., Liarzi, O., Shainskaya, A. & Eisenbach, M. (2008).** *In vivo* acetylation of CheY, a response regulator in chemotaxis of *Escherichia coli*. *J Mol Biol* **376**, 1260–1271.

**Yu, B. J., Kim, J. A., Moon, J. H., Ryu, S. E. & Pan, J. G. (2008).** The diversity of lysine-acetylated proteins in *Escherichia coli*. *J Microbiol Biotechnol* **18**, 1529–1536.

**Zhang, J., Sprung, R., Pei, J., Tan, X., Kim, S., Zhu, H., Liu, C. F., Grishin, N. V. & Zhao, Y. (2009).** Lysine acetylation is a highly abundant and evolutionarily conserved modification in *Escherichia coli*. *Mol Cell Proteomics* **8**, 215–225.

Edited by: G. Stewart